

Aminophosphines: A Double Role in the Synthesis of Colloidal Indium Phosphide Quantum Dots

Mickaël D. Tessier,^{*,†,‡,||} Kim De Nolf,^{†,‡,||} Dorian Dupont,^{†,‡} Davy Sinnaeve,[§] Jonathan De Roo,^{†,‡} and Zeger Hens^{*,†,‡}

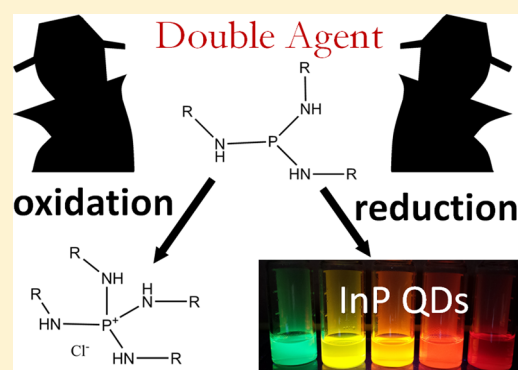
[†]Physics and Chemistry of Nanostructures, Ghent University, Ghent, Belgium

[‡]Center for Nano and Biophotonics, Ghent University, Ghent, Belgium

[§]NMR and Structural Analysis Unit, Ghent University, Ghent, Belgium

S Supporting Information

ABSTRACT: Aminophosphines have recently emerged as economical, easy-to-implement precursors for making InP nanocrystals, which stand out as alternative Cd-free quantum dots for optoelectronic applications. Here, we present a complete investigation of the chemical reactions leading to InP formation starting from InCl_3 and tris(dialkylamino)phosphines. Using nuclear magnetic resonance (NMR) spectroscopy and single crystal X-ray diffraction, we demonstrate that injection of the aminophosphine in the reaction mixture is followed by a transamination with oleylamine, the solvent of the reaction. In addition, mass spectrometry and NMR indicate that the formation of InP concurs with that of tetra(oleylamino)phosphonium chloride. The chemical yield of the InP formation agrees with this $4 \text{ P(+III)} \rightarrow \text{P(-III)} + 3 \text{ P(+V)}$ disproportionation reaction occurring, since full conversion of the In precursor was only attained for a 4:1 P/In ratio. Hence it underlines the double role of the aminophosphine as both precursor and reducing agent. These new insights will guide further optimization of high quality InP quantum dots and might lead to the extension of synthetic protocols toward other pnictide nanocrystals.



INTRODUCTION

Colloidal nanocrystals have many applications¹ ranging from optoelectronics^{2–4} to energy^{5–8} and catalysis.^{9,10} In particular, quantum dots (QDs) fluorescing in the visible range are of significant interest for lighting and display applications.^{11–14} In this respect, stringent restrictions on the use of cadmium in consumer products have initiated a shift from the well-characterized Cd-based QDs to Cd-free alternatives such as indium phosphide. The first synthesis of InP nanocrystals with a reasonable size dispersion was reported in 1995.¹⁵ This synthesis employed tris(trimethylsilyl)phosphine (PTMS) which remains hitherto the most widely used phosphorus precursor for the synthesis of InP QDs. However, this compound is in many respects problematic, as it is highly expensive and autoignites in contact with air. Recently, efficient protocols based on aminophosphines have been established to synthesize InP QDs of different sizes.^{16,17} As compared to PTMS, an aminophosphine precursor is inexpensive, is safe-to-use under ambient conditions, and has been proven to lead to InP QDs of comparable quality as the best samples obtained with PTMS.^{18,19} In addition, this aminophosphine-based synthesis can lead to InP/ZnE (E = S or Se) core/shell QDs that emit from 500 to 670 nm with an emission line width between 44 and 65 nm and a photoluminescence quantum yield of 20% to 80%.¹⁷

Since the early days of Cd-based QD syntheses, insights into the reaction mechanism were used to improve the synthetic result in terms of size control and minimization of size dispersion.²⁰ To date, several QD synthesis methods have been shown to follow a two-step process where the injected precursors first react to form the solute or monomer whose increasing concentration subsequently gives rise to nucleation and growth of nanocrystals.^{21–23} In this respect, mechanistic studies have addressed both the chemical reactions involved in monomer formation and the relation between the monomer formation rate and the size of the resulting nanocrystals.^{24–27} Especially in the case of CdSe QDs synthesized using trioctylphosphine selenium (TOP-Se), precursor conversion was investigated in great detail and found to consist of two essential steps, i.e., a coordination of TOP-Se to the Cd center, followed by the cleavage of the Se=P bond. Moreover, this precursor conversion was found to be limiting the overall rate of CdSe formation.²⁷ This finding not only resulted in several size tuning strategies^{24–26} but also indicated that a controlled synthesis of nanocrystals will only be possible if the precursor conversion is slow as compared to the nucleation and growth of the nanocrystals proper.

Received: February 3, 2016

Published: April 25, 2016

Importantly, such studies are shifting synthesis development from a semiempirical trial-and-error approach to a more rational design of synthesis protocols that allows for optimal control of the QD size and size dispersion. A recent and most striking example involves the formation of lead sulfide QDs from thiourea precursors where insight into the relation between reaction rate and nanocrystal size was implemented to achieve size control at full reaction yield over a broad range of nanocrystal diameters.²⁸ In the case of PTMS-based synthesis protocols for InP QDs, different mechanistic studies showed that precursor conversion is complete upon injection,^{29,30} resulting in ripening-driven nanocrystal growth. Although this was linked to the difficulty of synthesizing monodisperse InP QDs, the use of substituted silylphosphines with a lower reactivity did not overcome this problem.³¹ In the case of aminophosphine precursors on the other hand, the InP formation rate proved to be much slower.¹⁷ Whereas this lower rate was utilized to implement economical size-tuning-at-full-yield strategies, the chemistry of the conversion reaction is not yet understood. This, however, is crucial to further optimize the reaction and extend it to the synthesis of other metal phosphide and metal arsenide nanocrystals.

In this paper, we identify several key aspects that govern the formation of InP from aminophosphine precursors and indium chloride in the presence of primary amines. First, we show that the reaction involves the substitution of the original amino group by amines present in the reaction mixture, where only transamination with primary amines leads to InP formation. Furthermore, we find that the substituted aminophosphine has a double role in the reaction, serving as both the phosphorus precursor and the reducing agent by the formation of a P(V) phosphonium salt. These findings are summarized in a chemical reaction mechanism, that may help using this unique precursor chemistry for the formation of, e.g., GaP, InAs, or GaAs nanocrystals. These have proven even more challenging than InP to synthesize as nanocrystals, with synthesis methods suffering from poor size dispersions¹⁵ or requiring extremely hazardous precursors.^{32,33}

EXPERIMENTAL SECTION

Chemicals. Indium(III) chloride (99.999%), zinc(II) chloride ($\geq 98\%$), dodecylamine (99%), tris(diethylamino)phosphine (97%), tris(dimethylamino)phosphine (97%), selenium powder 100 mesh (99.99%), and zinc stearate (technical grade, 65%) were purchased from Sigma-Aldrich. Trioctylphosphine ($>97\%$) was purchased from Strem Chemicals. Oleylamine (80–90%) was purchased from Acros Organics (NB: Oleylamine is stored under an inert atmosphere). Octadecene (technical 90%) was purchased from Alfa Aesar.

Synthesis of Core/Shell InP/ZnSe QDs. 100 mg (0.45 mmol) of indium(III) chloride, as indium raw materials, and 300 mg (2.2 mmol) of zinc(II) chloride, as zinc raw materials, are mixed in 5.0 mL (15 mmol) of technical oleylamine which is a coordinating solvent. The reaction mixture is stirred and degassed at 120 °C for an hour and then heated to 180 °C under an inert atmosphere. Upon reaching 180 °C, a volume of 0.45 mL (1.6 mmol) of tris(diethylamino)-phosphine is quickly injected in the above-mentioned mixture. After the phosphorus precursor injection, the InP nanocrystals synthesis proceeded. The InP core QDs reaction occurs during 30 min. After 30 min, the shell growth procedure starts: slow injection of 1 mL of stoichiometric trioctylphosphine-selenium (2.2 M). At 60 min: the temperature is increased from 180 to 200 °C. At 120 min: slow injection of 1 g of Zn(stearate)₂ in 4 mL of octadecene. The temperature is increased from 200 to 220 °C. At 150 min: injection of 0.7 mL of stoichiometric trioctylphosphine-selenium (2.2 M). The temperature is increased from 220 to 240 °C. At 180 min: slow injection of 1 g of Zn(stearate)₂

in 4 mL of octadecene. The temperature is increased from 240 to 280 °C. At 210 min: slow injection of 0.7 mL of stoichiometric trioctylphosphine-selenium (2.2 M). The temperature is increased from 280 to 320 °C. After 240 min: slow injection of 1 g of Zn(stearate)₂ in 4 mL of octadecene. 300 min: end of reaction. At the end of the reaction, the temperature is cooled down. InP/ZnSe nanocrystals are then precipitated in ethanol and suspended in chloroform.

Mass Spectrometry (MS). InP core QDs are synthesized and precipitated with methanol. The supernatant is analyzed using a 6230 TOF-MS with ESI-source mass spectrometer from Agilent Technologies in a range from 55 to 1160 g·mol⁻¹.

NMR Spectroscopy. Aliquots of 40–100 μ L are taken from a synthesis and put into vials containing an inert atmosphere (Argon). It is crucial to prevent contact between aliquots and air. Oxidation of the aminophosphine species into aminophosphine oxide species leads to the appearance of extra resonances in the NMR spectra that complicate the interpretation. A fixed volume of the aliquots is dissolved in 500 μ L of toluene-d₈ (99.50% D, purchased at Eurisotop) and transferred to an NMR tube (5 mm). NMR measurements were recorded on a Bruker Avance III spectrometer operating at a ¹H frequency of 500.13 MHz and equipped with a BBI-Z probe or on a Bruker Avance II spectrometer operating at a ¹H frequency of 500.13 MHz and equipped with a TXI-Z probe (channels are ¹H, ¹³C, ³¹P). The sample temperature was set to 298.15 K. Quantitative ¹H spectra were recorded with a 20 s delay between scans to allow full relaxation of all NMR signals. The quantification was done by using the Digital ERETIC method. ³¹P spectra were recorded with 1H decoupling and a 20 s relaxation delay. Diffusion measurements (2D ³¹P DOSY) were performed using a double stimulated echo sequence for convection compensation and with monopolar gradient pulses.³⁴ Smoothed rectangle gradient pulse shapes were used throughout.

RESULTS AND DISCUSSION

In a typical aminophosphine-based synthesis of InP QDs, indium halides and zinc halides are dissolved in a primary amine as solvent (e.g., oleylamine, OlNH₂, where Ol = C₁₈H₃₅).^{16,17} The reaction mixture is subsequently degassed and heated to 150–220 °C, followed by the injection of tris(dimethylamino)phosphine, P(NMe₂)₃, or tris(diethylamino)phosphine, P(NEt₂)₃. Figure 1A depicts the UV–vis absorption spectra of different aliquots taken at various reaction times for the case of an InP QD synthesis at 180 °C (see Experimental Section for details). Already after 1 min of reaction, the first excitonic feature is clearly visible and its red shift with time points toward an increase of the QD diameter during the reaction. When the QDs reach their optimal size, shell precursors are added to the reaction mixture to obtain core/shell InP/ZnE (E = S, Se) QDs. In Figure 1A, the absorbance and photoluminescence spectra of InP/ZnSe QDs are shown. They have been obtained using stoichiometric trioctylphosphine selenium and zinc stearate mixed in octadecene as shell precursors (see Experimental Section for details). This sample exhibits a photoluminescence full width at half-maximum of 47 nm and a photoluminescence quantum yield of 50% which are excellent values in comparison to the best core/shell InP/ZnE QDs obtained with the PTMS precursor.^{18,19} Different size-tuning strategies, such as stopping the reaction before its end¹⁶ or using different indium halide or zinc halide precursors,¹⁷ allow obtaining InP/ZnE QDs over the entire visible range as shown in Figure 1B. A more extensive overview of absorbance and photoluminescence spectra of InP/ZnE with emission varying from 500 to 670 nm and their associated synthesis protocols are presented in the Supporting Information (see Supporting Information section S1).

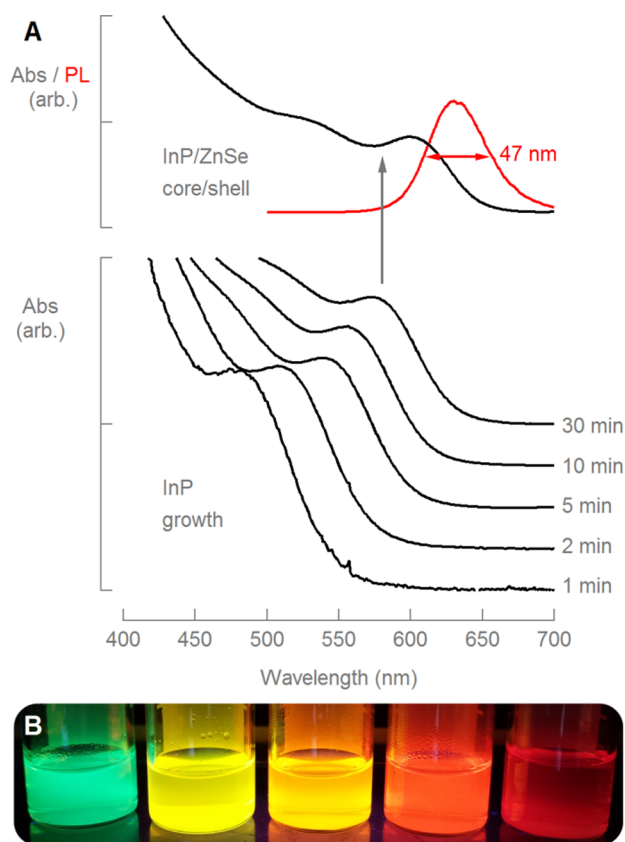


Figure 1. (A, bottom) Development of the absorption spectrum of InP QDs during a typical aminophosphine-based synthesis of InP QDs and (top) absorption and photoluminescence spectra of resulting InP/ZnSe QDs. (B) Picture of a series of different InP/ZnSe QDs emitting from 500 to 670 nm.

Although aminophosphines are excellent precursors for synthesizing InP QDs, they are not the most obvious. In PTMS, the phosphorus atom has an oxidation state of $-III$, rendering a reaction with an In(III) precursor such as indium chloride or indium acetate most likely. Aminophosphines on the other hand are P(III) compounds, such that intermediate reduction steps are needed to form InP in a reaction with an In(III) precursor. Two-step methods in which at least the indium precursor is reduced before reacting with the phosphorus precursor have already been described in the literature. $InCl_3$ for example can be reduced by KBH_4 to form $In(0)$ that then reacts with white phosphorus (P_4).³⁵ Another example is the reduction of $InCl_3$ by an organolithium reagent, followed by the reaction of the resulting $In(0)$ with triethylphosphine by a catalytic cleavage at high temperature.³⁶ Opposite from aminophosphine-based syntheses, however, such two-step strategies lead to rather polydisperse InP QDs. Alternatively, Song et al. hypothesized that InP formation starting from aminophosphine could involve the *in situ* formation of phosphine (PH_3) due to the presence of labile hydrogen in the primary amine solvent.¹⁶ However, with amines being poor Brønsted acids, such a mechanism seems unlikely.

To investigate possible intermediate reaction steps involved in the formation of InP out of aminophosphine and $InCl_3$, we first scrubbed the exhaust of an InP QD synthesis using a chemical gas trap (Figure 2A). Most notably, we observed the formation of a copper hydroxide precipitate upon scrubbing

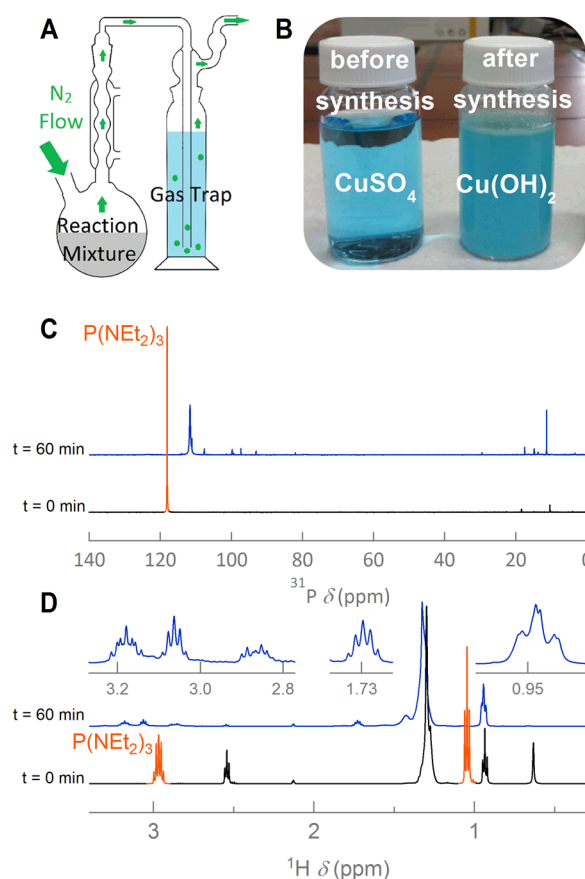


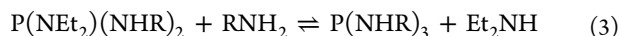
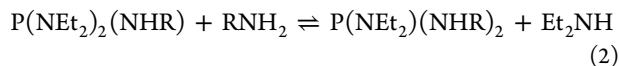
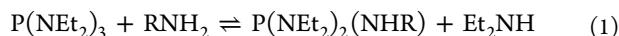
Figure 2. (A) Scheme of the gas trap mounting. (B) Picture of the $CuSO_4$ gas trap aqueous solution before and after an InP QDs synthesis. (C) ^{31}P NMR and (D) 1H NMR spectrum of $P(NEt_2)_3$ and dodecylamine, (black) prior to and (blue) after reaction at $120^\circ C$ for 60 min, together with a zoom on specific regions of the latter 1H spectrum. $P(NEt_2)_3$ resonances are indicated in orange.

with a saturated aqueous $CuSO_4$ solution, a strong indication that the exhaust contains a basic gas (Figure 2B). Scrubbing with a methanolic solution of hydrogen chloride enabled us to trap the base as a salt. After rotary evaporation, a solid residue was obtained, and following recrystallization in ethyl acetate, this salt was identified by single crystal X-ray diffraction as dimethylammonium chloride for a reaction where $P(NMe_2)_3$ was used as the phosphorus precursor (see Supporting Information section S2). This points toward an exchange between the amines used as a solvent in the synthesis and the amino groups of the original precursor. This exchange is also observed using $P(NEt_2)_3$ as the phosphorus precursor.

Simply mixing $P(NEt_2)_3$ and dodecylamine in a vial under an inert atmosphere confirms this transamination. Indeed, when the temperature is raised above $100^\circ C$, gas bubbles evolve, which we attribute to Et_2NH rather than $P(NEt_2)_3$, as the latter has a boiling point of $245^\circ C$. This is further corroborated by the two ^{31}P NMR spectra shown in Figure 2C, recorded on a mixture of $P(NEt_2)_3$ and dodecylamine prior to and 1 h after reaction. The initial solution features a single resonance of $P(NEt_2)_3$ at 118 ppm. This has almost completely vanished after 1 h of reaction due to transamination. Diethylamine is formed and has evaporated from the mixture (boiling point = $55^\circ C$). Moreover, a new, somewhat shifted dominant resonance appears at 111 ppm, most likely a transaminated

aminophosphine, next to several less intense resonances especially at around 11 ppm.

Denoting an alkyl moiety in general as R, this transamination can be written as a sequence of three successive reactions:



The ^1H NMR spectra prior to and after transamination presented in Figure 2D show again that the CH_3 and CH_2 resonances of $\text{P}(\text{NEt}_2)_3$ at 1.04 and 2.97 ppm disappear. In the region of the latter, three new resonances appear at 3.18, 3.07, and 2.86 ppm next to a fourth pentet resonance at around 1.73 ppm. These resonances come in an approximately 2:2:1:2 ratio. Such a ratio can be expected for the resonances of the two $\alpha\text{-CH}_2$, the N–H protons, and the $\beta\text{-CH}_2$ in the alkyl chain of a twice transaminated compound $\text{P}(\text{NEt}_2)(\text{NHR})_2$. Note that the CH_3 of the remaining NEt_2 group is shifted and almost overlaps with the CH_3 of the alkyl chain at around 0.95 ppm. A more detailed NMR analysis using $^1\text{H}\text{-}^{31}\text{P}$ HMBC (see Supporting Information section S3) confirms that the series of three resonances in the 3.2–2.8 ppm range is linked to the 111 ppm resonance in the ^{31}P spectrum. We thus assign this resonance to the $\text{P}(\text{NEt}_2)(\text{NHR})_2$ transaminated compound.

Transamination reactions for $\text{P}(\text{NMe}_2)_3$ and $\text{P}(\text{NEt}_2)_3$ have been described before.^{37,38} Burgada for example argued that an exchange between the dimethylamino group of $\text{P}(\text{NMe}_2)_3$ and a heavier second amino group can occur if the hydrogen of this second amino group is sufficiently labile.³⁷ As the boiling point of dimethylamine is 7.4 °C, this compound is eliminated from the reaction mixture after its formation, shifting the equilibrium of the reaction to the formation of a fully transaminated aminophosphine where the amino group has a higher boiling point than dimethylamine. Even if the author mentioned exchange between secondary amines only, it underlines our observation that a similar exchange involving a primary amine, such as dodecylamine or oleylamine, and a more volatile amino group, such as dimethylamino or diethylamino, occurs in the aminophosphine-based synthesis of InP.

The occurrence of transamination provides an important perspective on the role of the amino group in a particular aminophosphine precursor. First of all, it implies that adjusting this group to tune the precursor reactivity and thus the outcome of an InP synthesis risks to be an inefficient strategy if—as seems necessary—high boiling point amines are used as the solvent for the reaction. Indeed, in that case it will be the solvent that dictates what amino groups make up the true aminophosphine precursor. For one thing, this may explain why we do not observe significant differences in reactivity between, e.g., $\text{P}(\text{NMe}_2)_3$ and $\text{P}(\text{NEt}_2)_3$. On the other hand, the amino exchange highlights the role of the primary amine used as the solvent. By screening several amines, we find that InP is only formed when a primary amine is used. As listed in Table 1, no reaction takes place in the case of secondary or tertiary amines. This clearly indicates that primary amines are not just the solvent or the ligand in an aminophosphine-based InP synthesis. Rather, they must play a central role in the whole precursor chemistry.

Focusing on syntheses using $\text{P}(\text{NEt}_2)_3$ and InCl_3 in oleylamine, a key point to gain further insight into the

Table 1. Reaction Results As a Function of the Solvent Used

class	example	result
primary amines	butylamine	InP QDs
	octylamine	
	dodecylamine	
	oleylamine	
secondary amines	dioctylamine	no reaction
tertiary amines	trioctylamine	
other	trioctylphosphine	

precursor conversion is the observation we already made before that the conversion yield of the indium precursor into InP, i.e. the chemical yield, depends on the aminophosphine vs InX_3 equivalence.¹⁷ Here, the chemical yield is calculated by comparing the absorbance of quantitative aliquots with the intrinsic absorption coefficient of InP QDs at the same short wavelength.¹⁷ As shown in Figure 3, we find that the chemical

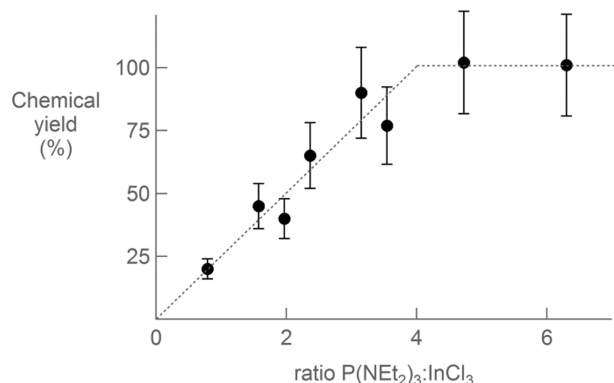
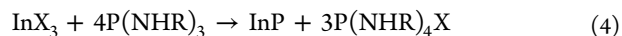


Figure 3. Conversion yield—amount of InP formed as fraction of the amount of InCl_3 used—of a tris(diethylamino)phosphine-based InP QDs synthesis plotted as a function of the $\text{P}(\text{NEt}_2)_3/\text{InCl}_3$ ratio used in the synthesis. The trend line is a straight line through the origin reaching full yield at a $\text{P}(\text{NEt}_2)_3/\text{InCl}_3$ ratio of 4, followed by a horizontal at 100% for higher $\text{P}(\text{NEt}_2)_3/\text{InCl}_3$ ratios.

yield increases proportionally to the $\text{P}(\text{NEt}_2)_3/\text{InX}_3$ molar ratio to reach 100% for ratios of ~ 4 or more. At this point, we hypothesize that a phosphorus precursor excess is needed to obtain full chemical yield because the aminophosphine plays more than one role in the synthesis. As discussed before, formation of InP from $\text{P}(\text{NEt}_2)_3$ comes with a reduction of P(III) to P(–III). One way to achieve this—and that accounts for the observed phosphorus excess needed to reach full conversion of the indium—is that 1 equiv of phosphorus is reduced to P(–III) by the oxidation of 3 equiv of phosphorus to P(+V). We have already demonstrated that injected $\text{P}(\text{NEt}_2)_3$ is modified during the synthesis by transamination. To continue this line of thought, we therefore propose an overall redox reaction in which 1 equiv of InP is formed by the oxidation of 3 equiv of the substituted aminophosphine to a phosphonium salt:



In this chemical equation, R represents an alkyl moiety of a primary amine and X is Cl, Br, or I.

The first evidence that eq 4 indeed describes the overall reaction leading to InP comes from the mass spectrum of the reaction mixture after removal of the InP QDs by methanol addition. As shown in Figure 4A, it contains three main

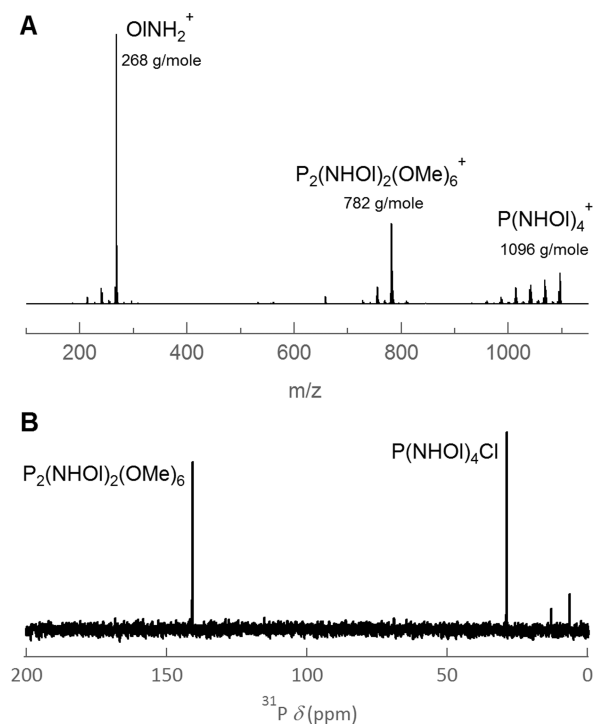


Figure 4. (A) Mass spectrum of the supernatant obtained after purification by methanol addition of a full yield diethylamino-phosphine-based InP QDs synthesis. (B) ^{31}P NMR spectrum of the supernatant used for mass spectrometry diluted using toluene- d_8 .

compounds. The first has a molar mass of 268 g/mol, most likely corresponding to oleylamine, which is the solvent of the reaction and thus is present in large amounts. The second compound has a molar mass of 782 g/mol, which corresponds to $\text{P}_2(\text{NHOL})_2(\text{OMe})_6$. Probably, this has been produced during the purification by a reaction between aminophosphine compounds and methanol (see [Experimental Section](#)). The third compound has a measured molar mass of 1096 g/mol which is close to the 1097 g/mol expected for $\text{P}(\text{NHOL})_4^+$, i.e., the oleylamino phosphonium cation generated by the reaction according to [eq 4](#).

To investigate in more detail this InP QD synthesis, we analyzed the reaction development using ^{31}P NMR spectroscopy. In [Figure 5A](#), the ^{31}P NMR spectra of the precursor mixture and reaction aliquots are shown. Five resonances can be distinguished. Next to the initial precursor at 118 ppm (P0), two more resonances appear at comparable chemical shifts of 111 (P1) and 98 (P2) ppm. Also in the case of transamination with oleylamine, the former can be related through ^1H - ^{31}P HMBC to a series of three ^1H resonances in the 2.8–3.2 ppm range that come with an approximately 2:2:1 intensity ratio (see [Supporting Information section S3](#)). Hence, we again attribute P1 to the twice transaminated compound $\text{P}(\text{NET}_2)_2(\text{NHOL})_2$. Also P2 couples to a ^1H resonance in the 2.8–3.2 ppm range (see [Supporting Information section S3](#)). As it always appears faster than P1 in a blank transamination reaction or during InP synthesis, we tentatively attribute this to the once transaminated compound $\text{P}(\text{NET}_2)_2(\text{NHOL})_1$. The resonance at 13 ppm (P3) exhibits a $^1J_{\text{PH}}$ coupling of 550 Hz, with the corresponding protons appearing at 7.42 and 6.31 ppm (see [Supporting Information section S3](#)). Such a P–H bond is typical for an iminophosphorane, which is made up of tautomers of aminophosphines with a primary amino group.³⁹

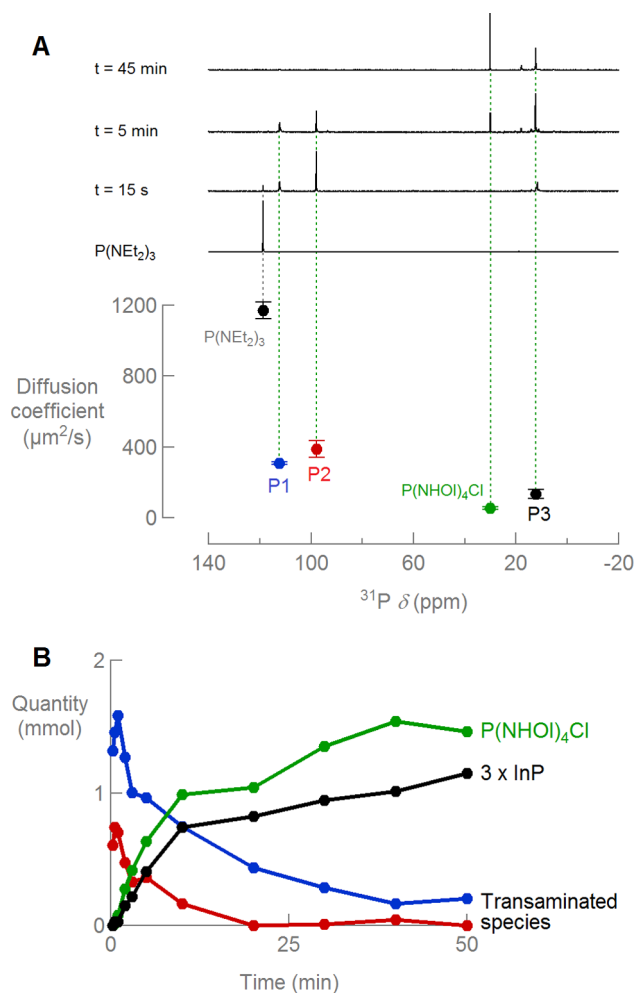


Figure 5. (A) (Top) ^{31}P NMR spectra of $\text{P}(\text{NET}_2)_3$ and different aliquots taken at the indicated time after initiating a diethylamino-phosphine based InP synthesis run at 170 °C, related to (bottom) the diffusion coefficient of the resonances as determined using ^{31}P DOSY. (B) (Colored) Concentration development of the prevailing species during a diethylamino-phosphine based InP synthesis run at 170 °C as estimated from ^{31}P NMR resonance intensities and (black) the concomitant amount of InP formed.

We therefore attribute P3 to a tautomer of one or more transaminated aminophosphines. Referring to [Figure 2c](#), a similar resonance appears in the blank transamination of $\text{P}(\text{NET}_2)_3$ by dodecylamine. Finally, we already identified the 29 ppm (P4) resonance as the phosphonium salt (see [Figure 4B](#)). Note that the assignment of P0, P1, P2, and P4 concurs with the variation of the diffusion coefficient of the corresponding compounds, which indeed gets smaller for the more bulky species (see [Figure 5A](#) and [Supporting Information section S4](#)).

By identifying P1 and P2 as transaminated species and P4 as the main reaction byproduct, the development of these different phosphorus species can be monitored during a reaction by analyzing successive aliquots; see [Figure 5B](#). Here, we derived the concentration of each species from the integrated intensity of its ^{31}P resonance. By taking a reaction carried out at 190 °C as an example, [Figure 5A](#) and [5B](#) show that 15 s after injection P0 has disappeared and the transaminated compounds are already the prevailing species. Importantly, this transamination is considerably sped up by the presence of InCl_3 and, especially, ZnCl_2 (see [Supporting](#)

Information section S5). Next, Figure S5 shows that, during the reaction, the concentration of $P(NHOL)_4Cl$ gradually increases at a rate concurring with the formation of InP with an estimated equivalence somewhat exceeding 3:1. Clearly, this observation confirms the overall chemical reaction eq 4, where indeed one InP equivalent is formed together with 3 equiv of $P(NHOL)_4Cl$ and it agrees with the MS analysis showing $P(NHOL)_4Cl$ to be the dominant reaction byproduct. The decrease in concentration of both transaminated aminophosphines follows the formation of InP, confirming their role as the actual phosphorus precursor in this reaction. More specifically, the absence of partially substituted phosphonium salts suggests that the actual precursor is most likely the fully transaminated compound $P(NHOL)_3$. Note that the concentration of the tautomeric form, on the other hand, stays largely constant during the reaction, suggesting that this P(V) compound is unreactive and only formed in the initial stage of the reaction.

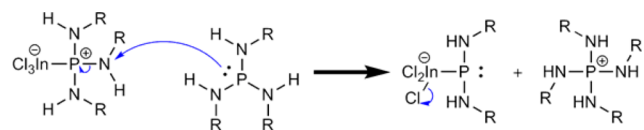
Based on the overall InP formation reaction expressed by eq 4, a chemical reaction mechanism can be proposed. In accordance with the double role of phosphorus, this mechanism assumes a nucleophilic attack by the phosphorus center of one aminophosphine on an amino group of another aminophosphine. Considering that the fully transaminated $P(NHR)_3$ is the actual reactant, Scheme 1–3 represent the different steps

Scheme 1. In–P Complex Formation



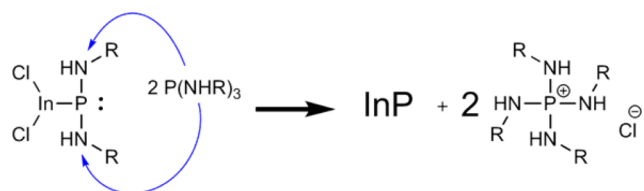
this conversion involves. In a first step (Scheme 1), an adduct of $InCl_3$ and $P(NHR)_3$ is formed. Importantly, such a complex exhibits different resonance structures (only two of which are shown), which lead to a delocalization of the positive charge over the phosphorus center and the surrounding nitrogen atoms. This renders the nitrogen atoms sensitive to a nucleophilic attack by a second $P(NHR)_3$ as represented in Scheme 2. This results in the formation of an InP intermediate

Scheme 2. Phosphorus Nucleophilic Substitution



and a first equivalent of the $P(NHR)_4Cl$ phosphonium salt. Note that this reaction leads to a first change in the phosphorus oxidation numbers, with that in the InP intermediate being reduced from +III to +I and that in the phosphonium salt being oxidized from +III to +V. Scheme 3 sketches subsequent

Scheme 3. InP Unit Formation



reduction steps, where two more equivalents of $P(NHR)_3$ further reduce the phosphorus in the InP intermediates to an oxidation state of –I and –III, respectively, and result in the formation of 1 equiv of InP. The proposed pathway provides an explanation as to why InP is only formed when using primary amines as the solvent. Indeed, steric hindrance may hamper both the formation of the adduct depicted in Scheme 1 and the subsequent nucleophilic attack on nitrogen. Moreover, an alkyl chain is an electron-donating group that can further stabilize the positive charge in the adduct. This may render the nitrogen atoms less electrophilic, a necessary attribute for the subsequent reactions.

CONCLUSION

In summary, we have studied the precursor conversion in the aminophosphine-based synthesis of InP QDs. We have shown that, upon injection, dimethyl- and diethylaminophosphine undergo rapid transamination with the amine used as the solvent. This leads to the release of dimethyl or diethylamine and an effective aminophosphine precursor that is the fully transaminated compound. Only in the case that primary amines are used, this leads to the eventual formation of InP, where a quaternary aminophosphonium salt is formed as the major reaction byproduct. This finding enables the overall InP formation reaction to be written as a redox reaction where 3 equiv of the transaminated aminophosphine reduce a fourth equivalent to form 1 equiv of InP. Importantly, this double role of the aminophosphine explains why full conversion of the In precursor into InP is only attained with a 4-fold excess of the aminophosphine. This picture is confirmed by monitoring the reaction development using ^{31}P NMR spectroscopy. Based on these findings, we propose a chemical reaction mechanism that involves a nucleophilic attack of one aminophosphine on the nitrogen in a second aminophosphine that is activated by complexation with $InCl_3$. We believe that the new chemistry introduced here for the formation of InP QDs may be extended to the formation of other III–V quantum dots, such as GaP, InAs, or GaAs, using similar aminophosphine or aminoarsine precursors.

ASSOCIATED CONTENT

Supporting Information

The Supporting Information is available free of charge on the ACS Publications website at DOI: 10.1021/jacs.6b01254.

InP/ZnS and InP/ZnSe QDs synthesis protocols, identification of dimethylamine gas by single crystal XRD, NMR analysis of the reaction between $P(NEt_2)_3$ and oleylamine, diffusion-ordered spectroscopy of the phosphorus prevailing species, comparison of the transamination rate for different protocols (PDF)

AUTHOR INFORMATION

Corresponding Authors

*mickael.tessier@ugent.be

*zeger.hens@ugent.be

Present Address

Krijgslaan 281, building S3 (Campus Sterre), 9000 Gent, Belgium.

Author Contributions

||M.D.T. and K.D.N. contributed equally.

Notes

The authors declare no competing financial interest.

ACKNOWLEDGMENTS

This work was funded by Instituut voor de Aanmoediging van Innovatie door Wetenschap en Technologie in Vlaanderen (IWT-SBO Lumicor). Z.H. acknowledges support by the European Commission via the Marie-Sklodowska Curie action Phonsi (H2020-MSCA-ITN-642656), the Belgian Science Policy office (IAP 7.35, photonics@be), and Ghent University (GOA 01G01513) for funding. J.D.R., K.D.N., and D.S. thank the Research Foundation—Flanders (FWO) for pre- and postdoctoral fellowships. The authors are grateful to Prof. J. C. Martins for the use of the 500 MHz NMR equipment (funded by The Hercules foundation), Prof. K. Van Hecke for the single-crystal diffraction, and Prof. F. Lynen for assistance with the mass spectrometry.

REFERENCES

- (1) Kovalenko, M. V.; Manna, L.; Cabot, A.; Hens, Z.; Talapin, D. V.; Kagan, C. R.; Klimov, V. I.; Rogach, A. L.; Reiss, P.; Milliron, D. J.; Guyot-sionnest, P.; Konstantatos, G.; Parak, W. J.; Hyeon, T.; Korgel, B. A.; Murray, C. B.; Heiss, W. *ACS Nano* **2015**, *9*, 1012.
- (2) Klimov, V. I. *Science* **2000**, *290*, 314.
- (3) Semonin, O. E.; Luther, J. M.; Choi, S.; Chen, H.; Gao, J.; Nozik, A. J.; Beard, M. C. *Science* **2011**, *334*, 1530.
- (4) Wang, X.; Koleilat, G. I.; Tang, J.; Liu, H.; Kramer, I. J.; Debnath, R.; Brzozowski, L.; Barkhouse, D. A. R.; Levina, L.; Hoogland, S.; Sargent, E. H. *Nat. Photonics* **2011**, *5*, 480.
- (5) Cadavid, D.; Ibáñez, M.; Gorsse, S.; López, A. M.; Cirera, A.; Morante, J. R.; Cabot, A. *J. Nanopart. Res.* **2012**, *14*, 1.
- (6) Ibáñez, M.; Korkosz, R. J.; Luo, Z.; Riba, P.; Cadavid, D.; Ortega, S.; Cabot, A.; Kanatzidis, M. G. *J. Am. Chem. Soc.* **2015**, *137*, 4046.
- (7) Osajca, M. F.; Bodnarchuk, M. I.; Kovalenko, M. V. *Chem. Mater.* **2014**, *26*, 5422.
- (8) Oh, M. H.; Yu, T.; Yu, S.-H.; Lim, B.; Ko, K.-T.; Willinger, M.-G.; Seo, D.-H.; Kim, B. H.; Cho, M. G.; Park, J.-H.; Kang, K.; Sung, Y.-E.; Pinna, N.; Hyeon, T. *Science* **2013**, *340*, 964.
- (9) De Roo, J.; Van Driessche, I.; Martins, J. C.; Hens, Z. *Nat. Mater.* **2016**, *15*, 517.
- (10) Shylesh, S.; Schünemann, V.; Thiel, W. R. *Angew. Chem., Int. Ed.* **2010**, *49*, 3428.
- (11) Bourzac, K. *Nature* **2013**, *493*, 283.
- (12) Chen, O.; Zhao, J.; Chauhan, V. P.; Cui, J.; Wong, C.; Harris, D. K.; Wei, H.; Han, H.-S.; Fukumura, D.; Jain, R. K.; Bawendi, M. G. *Nat. Mater.* **2013**, *12*, 445.
- (13) Rizzo, A.; Li, Y.; Kudera, S.; Della Sala, F.; Zanella, M.; Parak, W. J.; Cingolani, R.; Manna, L.; Gigli, G. *Appl. Phys. Lett.* **2007**, *90*, 051106.
- (14) Bae, W. K.; Park, Y.-S.; Lim, J.; Lee, D.; Padilha, L. a.; McDaniel, H.; Robel, I.; Lee, C.; Pietryga, J. M.; Klimov, V. I. *Nat. Commun.* **2013**, *4*, 2661.
- (15) Micic, O. I.; Sprague, J. R.; Curtis, C. J.; Jones, K. M.; Machol, J. L.; Nozik, A. J.; Giessen, H.; Fluegel, B.; Mohs, G.; Peyghambarian, N. *J. Phys. Chem.* **1995**, *99*, 7754.
- (16) Song, W.-S.; Lee, H.-S.; Lee, J. C.; Jang, D. S.; Choi, Y.; Choi, M.; Yang, H. *J. Nanopart. Res.* **2013**, *15*, 1750.
- (17) Tessier, M. D.; Dupont, D.; De Nolf, K.; De Roo, J.; Hens, Z. *Chem. Mater.* **2015**, *27*, 4893.
- (18) Xie, R.; Battaglia, D.; Peng, X. *J. Am. Chem. Soc.* **2007**, *129*, 15432.
- (19) Li, L.; Reiss, P. *J. Am. Chem. Soc.* **2008**, *130*, 11588.
- (20) Murray, C. B.; Norris, D. J.; Bawendi, M. G. *J. Am. Chem. Soc.* **1993**, *115*, 8706.
- (21) Deng, Z.; Cao, L.; Tang, F.; Zou, B. *J. Phys. Chem. B* **2005**, *109*, 16671.
- (22) Steckel, J. S.; Yen, B. K. H.; Oertel, D. C.; Bawendi, M. G. *J. Am. Chem. Soc.* **2006**, *128*, 13032.
- (23) Liu, H.; Owen, J. S.; Alivisatos, A. P. *J. Am. Chem. Soc.* **2007**, *129*, 305.
- (24) Abe, S.; Capek, R. K.; De Geyter, B.; Hens, Z. *ACS Nano* **2012**, *6*, 42.
- (25) Abe, S.; Capek, R. K.; De Geyter, B.; Hens, Z. *ACS Nano* **2013**, *7*, 943.
- (26) De Nolf, K.; Capek, R. K.; Abe, S.; Sluydts, M.; Jang, Y.; Martins, J. C.; Cottenier, S.; Lifshitz, E.; Hens, Z. *J. Am. Chem. Soc.* **2015**, *137*, 2495–2505.
- (27) Owen, J. S.; Chan, E. M.; Liu, H.; Alivisatos, A. P. *J. Am. Chem. Soc.* **2010**, *132*, 18206.
- (28) Hendricks, M. P.; Campos, M. P.; Cleveland, G. T.; Jen-La Plante, I.; Owen, J. S. *Science* **2015**, *348*, 1226.
- (29) Allen, P. M.; Walker, B. J.; Bawendi, M. G. **2010**, 760.
- (30) Gary, D. C.; Cossairt, B. M. *Chem. Mater.* **2013**, *25*, 2463.
- (31) Gary, D. C.; Glassy, B. A.; Cossairt, B. M. *Chem. Mater.* **2014**, *26*, 1734.
- (32) Guzelian, A. A.; Banin, U.; Kadavanich, A. V.; Peng, X.; Alivisatos, A. P. *Appl. Phys. Lett.* **1996**, *69*, 1432.
- (33) Cao, Y. W.; Banin, U. *J. Am. Chem. Soc.* **2000**, *122*, 9692.
- (34) Connell, M. A.; Bowyer, P. J.; Adam Bone, P.; Davis, A. L.; Swanson, A. G.; Nilsson, M.; Morris, G. A. *J. Magn. Reson.* **2009**, *198*, 121.
- (35) Yan, P.; Xie, Y.; Wang, W.; Liu, F.; Qian, Y. *J. Mater. Chem.* **1999**, *9*, 1831.
- (36) Lauth, J.; Strupeit, T.; Kornowski, A.; Weller, H. *Chem. Mater.* **2013**, *25*, 1377.
- (37) Burgada, R. *Bull. Soc. Chim. Fr.* **1963**, *10*, 2335.
- (38) Gopalakrishnan, J. *Appl. Organomet. Chem.* **2009**, *23*, 291.
- (39) Kolodyazhnyi, O. I.; Prinada, N. *Russ. J. Gen. Chem.* **2001**, *71*, 646.